Artículo original

Rev. Cubana Quím. e-ISSN: 2224-5421

Vol. 34, no. 3, septiembre-diciembre 2022

Theoretical predictions of doping strategies improving the transport properties of Li_2SnO_3

Predicciones teóricas de estrategias de dopaje para mejorar las propiedades de transporte del Li_2SnO_3

Rafael Francisco Mut-Benítez[1]https://orcid.org/0000-0002-0359-7098

E. Soto,[2]

Minh Tho-Nguyen[3]https://orcid.org/0000-0002-3803-0569

Yohandys A. Zulueta[4*]https://orcid.org/0000-0003-0491-5817

[1]Departamento de Física Aplicada, Facultad de Ciencias Naturales y Exactas, Universidad de Oriente, Santiago de Cuba, Cuba

[2]Departamento de Matemática, Facultad de Ciencias Naturales y Exactas, Universidad de Oriente, Santiago de Cuba, Cuba

[3]Institute for Computational Science and Technology (ICST), Ho Chi Minh City, Vietnam

[4]Departamento de Física, Facultad de Ciencias Naturales y Exactas, Universidad de Oriente, Santiago de Cuba, Cuba

[*]Corresponding author email: yzulueta@uo.edu.cu

ABSTRACT

Nowadays, one of the primary worldwide challenges is the replacement of conventional fossil fuels by different renewable energy sources. The search for suitable solutions is getting more urgent in view of the severe consequences of the climate change the distribution of energy resources. Lithium stannate (Li_2SnO_3) is one of the battery material used as electrode and inorganic solid electrolyte. In this work, advanced atomistic simulations were performend to disclose the defect energetics behavior and large scale transport properties of pristine and metal doped Li_2SnO_3. The results of defect energetics computations show that divalent dopants occupies the Li site, leading to Li vacancy formation is a viable incorporation mechanism. In contrast, trivalent dopants have a strong energetic preference for doping at the Sn site, with charge compensation from Li interstitial formation. The results of molecular dynamics simulations disclose improvements of transport properties of Li_2SnO_3 upon doping strategies are observed.

Keywords: Li_2SnO_3; Li-ion battery; alkali-ion battery; atomistic simulations; Li-ion migration.

RESUMEN

Actualmente, una de las prioridades globales es el reemplazo del uso de combustibles fósiles por fuentes de energía renovables. La búsqueda de soluciones viables se está convirtiendo en un problema urgente, teniendo en cuenta el cambio climático y la actual distribución de fuentes de energía. El estannato de litio (Li_2SnO_3) es uno de los materiales usados en baterías de litio como electrodo o electrolito inorgánico. En este trabajo se emplean simulaciones atomísticas avanzadas para estudiar el efecto del dopaje con metales sobre las propiedades de transporte y la formación de defectos. Los resultados muestran que los dopantes divalentes, al ocupar los sitios del Li, crean sitios adiciones de vacancias de Li. Los dopantes trivalentes prefieren ocupar los sitios del Sn, creando ocupación de Li en los intersticios. Los resultados de las simulaciones, empleando dinámica molecular, muestran las estrategias de dopaje para mejorar las propiedades de transporte del Li_2SnO_3.

Palabras clave: Li_2SnO_3; batería de ion Li; batería alcalina; simulaciones atomísticas; migración de Li.

Recibido: 28/5/2022 Aprobado: 25/6/2022

Introduction

In the context of a global transition to cleaner energy technologies, the design of safer, more durable energy storage devices constitutes an urgent research subject. Replacing the liquid electrolytes traditionally used in batteries with solid-state electrolytes (SSE) is a promising route to overcome existing issues associated with current liquid-electrolyte batteries, including flammability, leakages, and volatility. However, the development of inorganic SSE faces critical challenges, such as relatively low ionic conductivity as compared to conventional liquid electrolytes, interfacial resistance with the electrodes, and a narrow electrochemical window, which constrains their practical applications.(1)

Outstanding ion transport, recognized by high diffusion coefficients of the lithium ions and low activation energies, is an essential requirement of a material to be considered as an electrolyte for LIBs.(1-5) Lithium stannate, Li_2SnO_3, is considered for many energy storage applications, including as an electrode, a inorganic solid electrolyte and a coating material for anodes in Li-ion batteries.(5)

Atomistic simulations based on density functional theory (DFT) and forcefield approaches have previously been used to explore the ground-state properties of undoped and doped Li_2SnO_3.(3, 4, 6, 7) Advanced atomistic simulations disclose additional information to experiment, related to revealing the migration mechanisms and energetics of dopant incorporation. Kuganathan *et al*.(3) studied defect formation and ion migration in Li_2SnO_3 and showed that dopant with 4+ valence charge are the best dopants to be incorporated at the Sn^{4+} site in terms of lowering the formation energy.(3) Al^{3+} as a dopant can also be used to occupy the Sn^{4+} site to increase the Li concentration in Li_2SnO_3 via Li interstitial defect compensation. The activation energy of Li-ion migration through various diffusion paths were also evaluated by using the conventional transition state theory.(3)

In our recent works, the defect formation energy and transport properties of transition metal dopant and pure divalent dopant were studied in two separated papers.[6, 7] Besides, the information collected in those manuscript are inaccessible for the majority of the researcher in the field living in developing countries. Collecting the main results of those manuscript, the aim of this work consists in the exploration of the ion transport properties and capabilities of Na- and K-doped Li_2SnO_3 as an inorganic solid electrolyte using advanced atomistic simulations. Defect formation and ion migration in Li_2SnO_3 systems are investigated, revealing the potential of Na- and K-doped Li_2SnO_3 as a promising inorganic solid electrolyte material.

Methodology

Lattice static calculations are performed using the GULP code.[8] Interatomic potential parameters to model the ion interactions are taken from the literature.[6, 7] The Mott–Littleton approach is used for the defect calculations.[9] This method subdivides the crystal structure into two spherical regions with radius r1 and r2 (with r1<r2), respectively. The isolated defect or defect cluster is located at the inner sphere r1, where the interaction between the defect/cluster with the local structure is strong. The external region r2 is treated by a quasi–continuum approximation.[9] To the best accuracy of the defect energetics calculations, values of r1 = 13 Å and r2 = 21 Å are assumed after convergence testing. The Broyden–Fletcher–Goldfarb–Shanno algorithm was adopted to update the cell parameters and fractional positions during the defect energetics and geometry optimizations computations.[8] This technique has been used to explore ion migration and defect formation in solid-state materials.[6,7,10,11]

LAMMPS code is used to determine the long-range diffusion of Li ions via potential–based MD simulations.[12] The simulation boxes were created using a 5×5×4 supercell of Li_2SnO_3, equivalent to 4800 ions in the stoichiometric cell. The temperature range for MD simulations is 500–1 100 K. We consider two kinds of defective Li_2SnO_3 supercells; the first one contemplates the common Li_2O Schottky defect and the second, the incorporation of divalent dopants as additional source of Li vacancies. The simulation boxes were first relaxed using an isothermal–isobaric ensemble (NTP) for reaching the equilibrium, the production runs were carried out with an isothermal-isochoric ensemble (NVT), while recording the mean square displacement (MSD) for the Li ions. The slope of the expected straight line of MSD plots was then used to calculate the diffusion coefficients (D) by the equation:

$$\square MSD = 6Dt \qquad /1/$$

where t is the simulation time. Given the significant number of defect concentrations, each production run was limited to 2 nanoseconds (ns) with a time step of 2 faraseconds (fs).

Results and discussion

In order to disclose the transport properties, we consider various incorporation mechanisms: Li_2O Schottky defect formation in pristine Li_2SnO_3, divalent dopant (M^{2+}) at the Li -site with a Li -vacancy formation ($M_{Li}^{\bullet} - V_{Li}'$), the substitution of M^{2+} at the Sn -site leading oxygen vacancy ($M_{Sn}'' - V_O^{\bullet\bullet}$). For trivalent dopants (M^{3+}) various incorporation schemes were considered, involving Li interstitial, and partial substitution of trivalent dopant at Li- and Sn- site leading Li and oxygen vacancies.[6, 7]

The first mechanism describes Li_2O Schottky defect formation in pristine Li_2SnO_3:

$$2Li_{Li} + O_O \rightarrow 2V_{Li}' + V_O^{\bullet\bullet} + Li_2O \qquad (1)$$

where Li_{Li} is a Li –ion at a Li –site, O_O is an O –ion at an O –site and V_{Li}' ($V_O^{\bullet\bullet}$) represents a Li (O) vacancy. The second scheme represents the incorporation mechanism of a divalent dopant (M^{2+}) at the Li –site with a Li –vacancy formation to ensure the charge neutrality:

$$MO + 2Li_{Li} \rightarrow M_{Li}^{\bullet} + V_{Li}' + Li_2O \qquad (2)$$

where $M_{Li}^{\bullet}$ denotes a divalent dopant occupying a Li –site in Li_2SnO_3 lattice structure. Furthermore, the substitution of M^{2+} at the Sn –site is described by equation (3):

$$MO + Sn_{Sn} + O_O \rightarrow M_{Sn}'' + V_O^{\bullet\bullet} + SnO_2 \tag{3}$$

where M_{Sn}'' represents a M^{2+}–dopant at the Sn –site.

In this study, three incorporation mechanisms involve trivalent dopants (M^{3+}) are additionally considered:

$$M_2O_3 + 6Li_{Li} \rightarrow 2M_{Li}^{\bullet\bullet} + 4V_{Li}' + 3Li_2O \tag{4}$$

$$M_2O_3 + 2Sn_{Sn} + O_O \rightarrow 2M_{Sn}' + V_O^{\bullet\bullet} + 2SnO_2 \tag{5}$$

$$M_2O_3 + 2Sn_{Sn} + Li_2O \rightarrow 2M_{Sn}' + 2Li_i^{\bullet} + 2SnO_2 \tag{6}$$

Equation (6) deals with M^{3+} substitution at the Sn–site occupying interstitial sites ($Li_i^{\bullet}$) in the structure. The solution (E_s), binding (E_B) and final solution (E_f) energies are computed accordingly. The solution energy (E_s) for the defect energy for the Li_2O Schottky defect is defined by equation (8):

$$E_s = \frac{1}{3}\left(2E_{vac}^{Li} + E_{vac}^{O} + E_L^{Li_2O}\right) \tag{7}$$

where E_{vac}^{Li}, E_{vac}^{O} and $E_L^{Li_2O}$ represent the required energy for a Li (O) –vacancy creation (in eV/defect) and the lattice energies of Li_2O (in eV/uc), respectively.

For the M^{2+} incorporation at Li– and Sn– site the relations are:

$$E_s = E_{Li}^{M^{2+}} + E_{vac}^{Li} + E_L^{Li_2O} - E_L^{MO} \tag{8}$$

$$E_s = E_{Sn}^{M^{2+}} + E_{vac}^{O} + E_L^{SnO_2} - E_L^{MO} \tag{9}$$

respectively. In equations (8) and (9) $E_{Li}^{M^{2+}}$, $E_{Sn}^{M^{2+}}$ denote the M^{2+} substitution energy at the Li– and Sn– site (in eV/dopant) and E_L^{MO}, $E_L^{SnO_2}$ the lattice energy of the MO and SnO_2 oxides, respectively. In the case of trivalent dopant, the solution energy is given by:

$$E_s = \frac{1}{2}\left(2E_{Li}^{M^{3+}} + 4E_{vac}^{Li} + 3E_L^{Li_2O} - E_L^{M_2O_3}\right) \tag{10}$$

$$E_s = \frac{1}{2}\left(2E_{Sn}^{M^{3+}} + E_{vac}^{O} + 2E_L^{SnO_2} - E_L^{M_2O_3}\right) \tag{11}$$

$$E_s = \frac{1}{2}\left(2E_{Sn}^{M^{3+}} + E_{int}^{Li} + 2E_L^{SnO_2} - E_L^{Li_2O} - E_L^{M_2O_3}\right) \tag{12}$$

where $E_{Li}^{M^{3+}}$ denotes the M^{3+} substitution energy at Li –site, E_{int}^{Li} at interstitial atomic position, $E_{Sn}^{M^{3+}}$ at the Sn –site and $E_L^{M_2O_3}$ the lattice energy of the M_2O_3 oxide considered. Figure 1 depicts the results of defect energetics computations. For the Li_2O Schottky defects, the formation leads to 2 eV/defect, which agrees with the reported values in the literature.[(3, 6, 7)] Solution energy varies from 1,84 to 2,80 eV/dopant for M^{2+} at the Li -site leading a Li vacancy. Mn^{2+}, Sc^{2+} and Cd^{2+} have the lowest E_s and E_f values. In this sense, these dopants are favorable to control the Li-vacancy concentration with low energetic cost. For the binding energy analysis, all E_B values are negative, indicating the effective defect formation cluster relative to the incorporation mechanisms in concern.

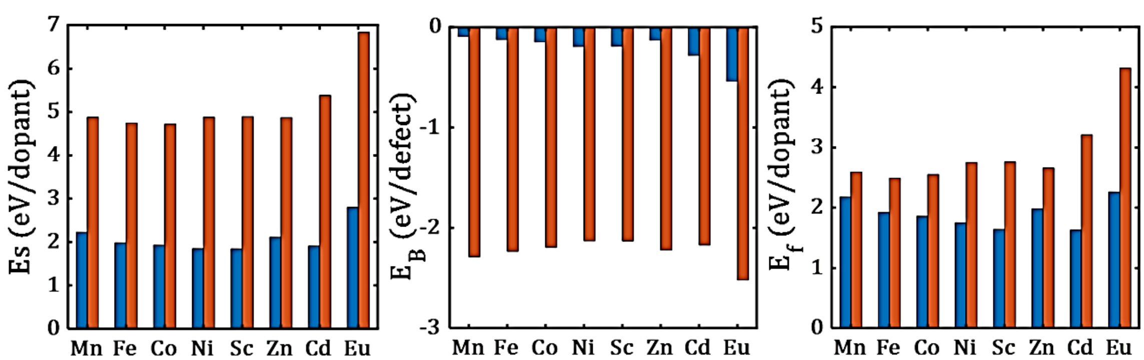

Fig. 1- Solution (Es), binding (E_B) and final solution (E_f) energy of M^{2+} at a Li-site leading one Li-vacancy (blue bars) and M^{2+} at a Sn-site leading oxygen vacancy (brown bars), respectively

Figure 2 shows the defect energetic behavior for transition state dopant, specifically for 3+ charge state. Li- interstitial mechanism have lower E_S and E_f, which indicates that trivalent dopants have a strong energetic preference for doping at the Sn-site, with a charge compensation from Li-interstitial formation. For binding energy, the values are similar to those obtained for divalent dopants.

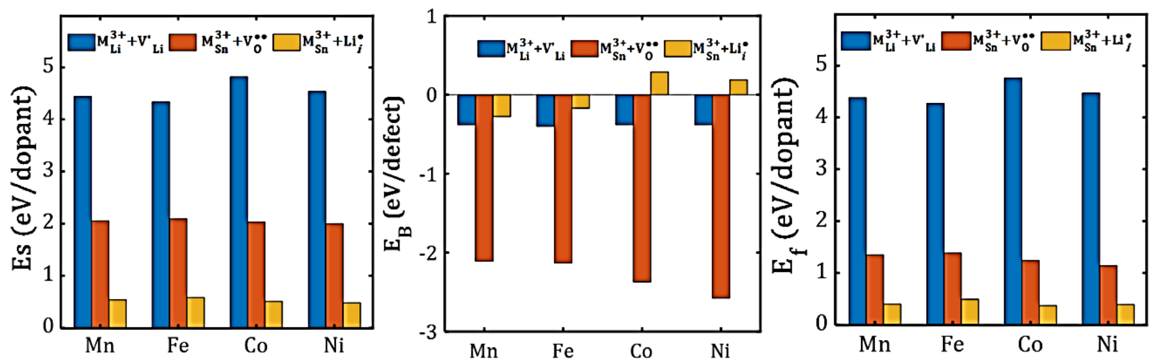

Fig. 2- Solution (Es), binding (E_B) and final solution (E_f) energy of (blue bars) for transition metal dopant incorporation mechanisms. The legend depicts the pair defect involved

Inclusion of divalent dopant at Li site creates strong attractive interactions as compared to the repulsive Li–Li pair, while the interaction becomes even stronger for $M''_{Sn} - V_O^{\bullet\bullet}$. Fe^{2+}, Co^{2+} and Zn^{2+} emerged as the best dopants to control the oxygen vacancy concentration, whereas Sc^{2+} and Cd^{2+} are good for tracking the Li-vacancy concentration in divalent doped Li_2SnO_3.

The transport properties of doped Li_2SnO_3 samples were evaluated.(6,7) Figure 3 displays calculated results of the Arrhenius-type dependence of diffusion and dc-conductivity for the specific divalent dopant samples. The results pointed out that the diffusion coefficient is higher in one or two orders of magnitude as compared to the non-doped sample where the Li-interstitial defect is involved.(7) In the latter case, transport properties of monocrystalline samples are exposed. The Li-interstitial mechanism leads to the highest diffusion coefficient as a consequence of a reduction of the average Li-Li distance, improving the Li-migration with smaller activation energy. As Co^{3+} and Mn^{3+} have the lowest Ea values upon charge state and relatively low final solution energy, both dopants can be considered to improve the transport properties as found in the resulting transition metal doped Li_2SnO_3 samples.

For pure divalent dopants, the corresponding transport properties, diffusion coefficient and dc-conductivity (σ) are also evaluated. For this set of divalent dopants, transport properties are evaluated for both mono- and nanocrystalline Li_2SnO_3 doped samples.[(6)] The results are displayed in figure 4. As it is shown in figure 4, in monocrystalline divalent-doped Li_2SnO_3, the Sc^{2+}, Zn^{2+}, Cd^{2+} and Eu^{2+} dopants can result in a Li-ion diffusion/conduction improvement of over one order of magnitude in contrast to the pristine Li_2SnO_3 sample with low activation energies.[7] The activation energy ranges between 0,40-0,44 eV and 0,34-0,38 eV for diffusion and conduction, respectively. Zn^{2+} is the best candidate to be used for improvement of the transport properties in monocrystalline Li_2SnO_3. A favorable reduction of the activation energy of 0,39-0,43 eV and 0,33-0,36 eV for diffusion and conduction, respectively, is observed. Activation energies are smaller in polycrystalline samples except for Zn^{2+} doped sample.[(6)] These findings imply that Li ion transport properties can effectively be improved upon doping with divalent dopants, leading to better battery performance of polycrystalline samples.[(6,7)]

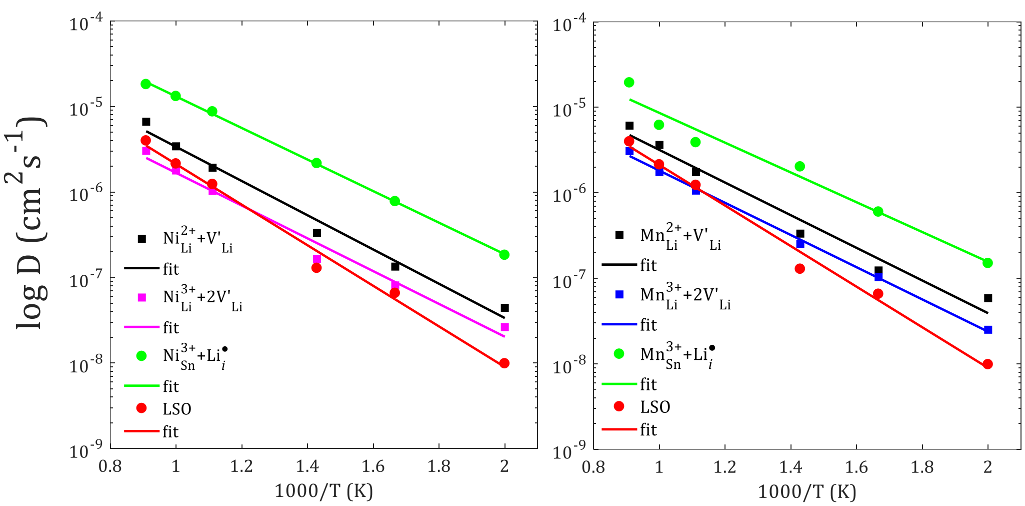

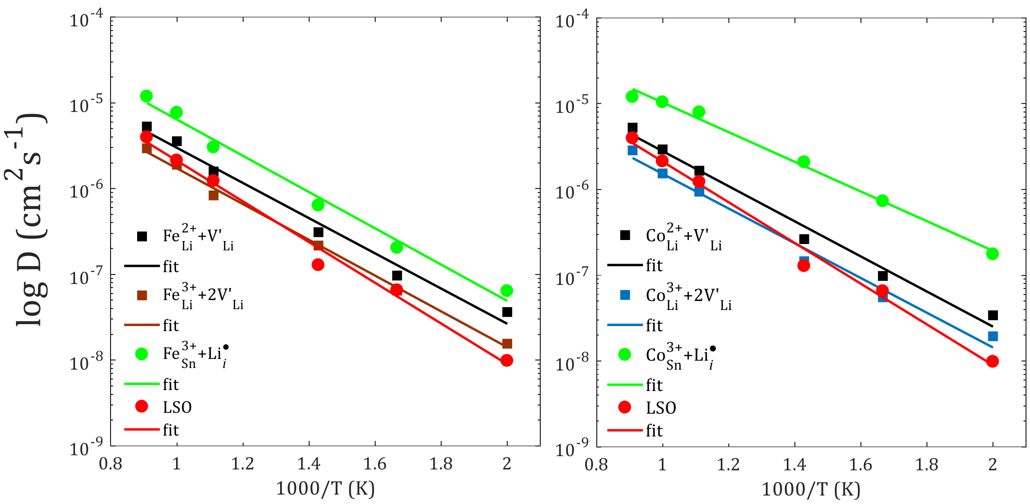

Fig. 3- Arrhenius plot of Li diffusion coefficient for each sample. LSO denotes the Schottky defect mechanism

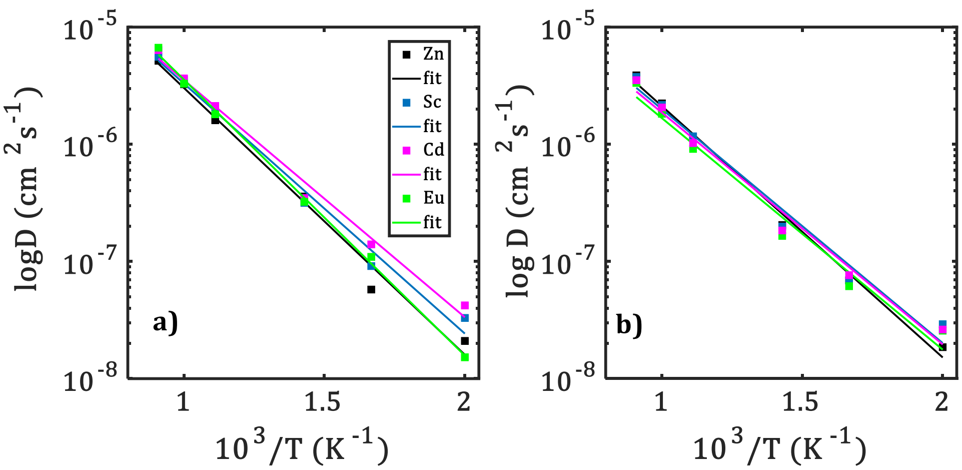

Fig. 4- Arrhenius dependence of **a)-b)** Li-ion diffusion coefficient (D) with the temperature (T) of mono- and polycrystalline M^{2+}-doped Li_2SnO_3 (M^{2+} = Zn^{2+}, Sc^{2+}, Cd^{2+} and Eu^{2+}) samples, respectively

Combination of calculated results of defect energetics and transport properties points out that inclusion of transition metal and pure divalent dopant into the Li_2SnO_3 structure effectively improves the quality of transport properties of Li_2SnO_3 with direct improvement for electrode/electrolyte in alkali ion batteries.[6, 7]

Conclusions

We have utilized atomic-scale simulations to study dopant incorporation and Li –ion diffusion in pristine and metal doped Li_2SnO_3. Defect energy calculations reveal that divalent dopants occupies the Li site, leading to Li vacancy formation. In contrast, trivalent dopants have a strong energetic preference for doping at the Sn site, with charge compensation from Li –interstitial formation. Molecular dynamics simulations show that transition metal doped Li_2SnO_3 can result in a Li ion diffusion enhancement with lower activation energies. The activation energy for diffusion ranges between 0,34–0,42 eV, while the undoped value is 0,48 eV. In fact, trivalent states of transition metal dopant reduce the activation energy as compared with divalent state and undoped samples. Of particular interest, the interstitially Li containing samples have better transport properties as compared with the other samples. The values reported here are in line with those reported for other similar Li ion conductor compounds.

Based on the results of defect formation and transport properties explored in this work, we believe that divalent/trivalent doped Li_2SnO_3 can be proposed as a candidate material for electrodes and inorganic solid state electrolytes in alkali –ion batteries.

Bibliographic references

1. AHNIYAZ, A. *et al.* "Progress in Solid-State High Voltage Lithium-Ion Battery Electrolytes." *Advances in Applied Energy*. **19**, 2021, 100070. ISSN 26667924.

2. WANG, Q.; HUANG, Y.; ZHAO, Y.; ZHANG, W.; WANG, Y. "Preparation of Li_2SnO_3 and Its Application in Lithium-Ion Batteries." *Surf. Interface Anal.* 2013, **45**, 1297–1303. ISSN 10969918.

3. KUGANATHAN, N.; KORDATOS, A.; CHRONEOS, A. "Li_2SnO_3 as a Cathode Material for Lithium-Ion Batteries: Defects, Lithium Ion Diffusion and Dopants." *Sci. Rep.* 2018, **8** (1), 3–11. ISSN 20452322.

4. ZULUETA, Y. A.; NGUYEN, M. T. Lithium Hexastannate: A Potential Material for Energy Storage. *Phys. Status Solidi B.* 2018, **255** (7), 1–9. ISSN 15213951.

5. YANG, S. *et al*. "Li_2SiO_3@Li_2SnO_3/SnO_2 as a High Performance Lithium-Ion Battery Material." *Mater. Lett.* 2019, **234**, 375–378. ISSN 02728842.
6. ZULUETA, Y. A.; NGUYEN, M. T. "Enhanced Li-Ion Transport in Divalent Metal-Doped Li_2SnO_3." *Dalt. Trans.* 2021, **50** (8), 3020–3026. ISSN 14779234.
7. ZULUETA, Y. A.; NGUYEN, M. T.; DAWSON, J. A. "Boosting Li-Ion Transport in Transition-Metal-Doped Li_2SnO_3." *Inorg. Chem.* 2020, **59** (16), 11841–11846. ISSN 1520510X.
8. GALE, J. D.; ROHL, A. L. "The General Utility Lattice Program (GULP)." *Mol. Simul.* 2003, **29**, 291–341. ISSN 08927022.
9. MOTT, N. F.; LITTLETON, M. J. "Conduction in Polar Crystals. I. Electrolytic Conduction in Solid Salts." *Trans. Faraday Soc.* 1938, **34**, 485–499. ISSN 00147672.
10. ZHANG, B.; LIN, Z.; WANG, L.-W.; PAN, F. "Achieving Both High Ionic Conductivity and High Interfacial Stability with the $Li_{2+x}C_{1-x}B_xO_3$ Solid-State Electrolyte: Design from Theoretical Calculations." *ACS Appl. Mater. Interfaces.* 2020, **12** (5), 6007–6014. ISSN 19448244.
11. DAWSON, J. A.; CANEPA, P.; FAMPRIKIS, T.; MASQUELIER, C.; ISLAM, M. S. "Atomic-Scale Influence of Grain Boundaries on Li-Ion Conduction in Solid Electrolytes for All-Solid-State Batteries." *J. Am. Chem. Soc.* 2018, **140** (1), 362–368. ISSN 15205126.
12. PLIMPTON, S. "Fast Parallel Algorithms for Short-range Molecular Dynamics." *J. Comput. Phys.* 1995, **117**, 1–19. ISSN 00219991.

Conflict of interest

The author have no conflict of interest to declare.

Authors contributions

The authors contributes equality to the conception and preparation of the manuscript.

Financial support

This research was conducted with the support of the Cuban Centre for Academic Supercomputing (HPC-Cuba) supported by the VLIR-UOS JOINT project and the Iberoamerican Supercomputing Network (RICAP).